

## Experimental and Computational Analysis of Fuel Mixing in a Low Pressure Direct Injection Gasoline Engine

Shalabh Srivastava<sup>\*</sup>, Farhad A. Jaber, Harold J. Schock, and David L.S. Hung  
Department of Mechanical Engineering  
Michigan State University  
East Lansing, MI 48824 USA

### Abstract

An experimental and computational investigation of the fuel spray mixing in an optically accessible single-cylinder direct-injection engine under realistic operating conditions was performed. High speed flow visualization in the optical engine was performed with images taken at a rate of 10,000 frames per second. The numerical simulations were carried out using the KIVA-3V software, which uses the discrete particle method for modeling the spray, with the secondary droplet breakup modeled by the Taylor Analogy Breakup (TAB) model. The nozzle configuration, jet orientation, injection flow rate and other injection parameters were matched with the experimental conditions. The simulated spray patterns in the cylinder were shown to compare well with the fuel distribution images obtained from the high speed flow visualization. The computational and experimental results for the fuel impingement on the cylinder walls, piston and valves, and those for the spark plug wetting and evaporated fuel mixing indicate the strong dependency of the fuel-air mixing to the spray pattern.

---

### Introduction

In order to meet more stringent fuel efficiency and vehicle emission standards and regulations, automotive engineers and researchers have recently focused on the development of innovative engine combustion and powertrain subsystems. Among many key technologies developed for the improvement of gasoline engines, one may refer to new direct fuel injection concepts. The fuel spray quality including the spray shape, the fuel penetration, the drop size distribution, the dynamic flow stability and repeatability have been identified as key factors in the control of the combustion efficiency and exhaust gas emissions in new engines. In this work, experimental and computational methods have been used for studying the in-cylinder fuel-air mixture formation process and the effect of injector spray pattern on this process in a direct-injection gasoline engine.

### Experimental and Computational Methods

The experiments were carried out in an optically accessible single-cylinder engine with two intake valves and one exhaust valve. The employed Low Pressure Direct Injection (LPDI) fuel delivery system [1, 2] consisted of a specially designed “high-turbulence” fuel injector with multi-hole nozzles. Such a multi-hole fuel injector has an advantage over existing fuel injectors as the number of holes, their pattern and orientation, and the internal flow cavity can be controlled individually to generate different overall spray patterns, allowing high flexibility. In this study, three different configurations with 8 holes and one configuration with 6 holes were considered. The 6-hole nozzle had a custom made spray pattern, with holes of different sizes. The 8-hole configurations had overall spray angles of 40, 60 and 80 degrees, with offsets of 0, 5 and 10 degrees from the injector axis and are denoted as 40/0, 60/5 and 80/10, respectively. These sprays had the same basic 8-hole nozzle configuration, but different internal geometrical configurations were employed which produced different overall spray angles and offset angles. In order to verify the spray configurations, the spray geometrical parameters like spray angle, offset angle, and spray tip penetration were obtained from the Mie-scattered images. The Sauter Mean diameter (SMD) of the droplets was measured using Phase Doppler Interferometry, while the injector dynamic flow rate was measured using an automated injector flow stand, as described in Ref. [3]. The outlines of the three injector spray orientations along with the orientation and mounting locations for the injector and the spark plug are shown in Figure 1. The injector is inclined at an angle of 35° with respect to the horizontal axis. The figure also shows the Mie-scattered images of three spray patterns.

The high speed flow visualization in the optical engine was performed with the collection of images at different planes taken at a rate of 10,000 frames per second. The liquid phase was visualized using a Mie-scattering tech-

---

<sup>\*</sup>Corresponding author

nique. Only the 8-hole nozzle configurations were studied. The amount of fuel injected was controlled by the injection pulse width to create a stoichiometric fuel-air mixture in the cylinder after complete evaporation and mixing. In-cylinder fuel distributions were obtained at crank angle intervals of  $1.5^\circ$ . The fuel impingement on the cylinder wall was characterized by computing the local and overall fuel impingement indexes via image processing algorithms, utilizing the intensity of the image pixels. The details of the experimental setup and measurements are given in Ref. [3].

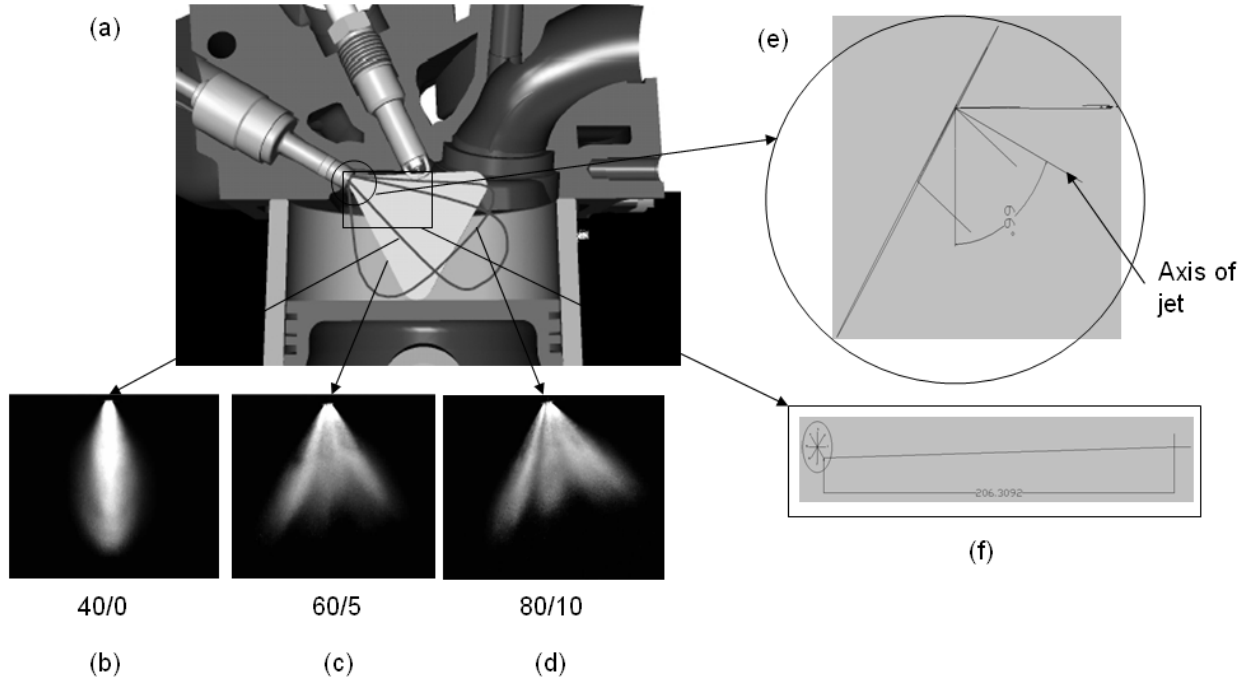


**Figure 1.** (a) Cross sectional view of the cylinder head, (b), (c), and (d), Mie-scattered spray images of the 8-hole nozzle configurations, (e) and (f) CAD figures used to model the nozzle configuration and spray in the numerical simulations.

Numerical simulations were carried out using KIVA-3V, a widely used, open source CFD code [4, 5, 6, 7]. In KIVA-3V, a discrete Lagrangian particle method is used for the modeling of fuel spray. Each computational particle represents a group of droplets with same size, velocity and temperature. A Monte Carlo sampling technique is used to determine the properties of the droplets at the injection and downstream locations. The governing equations describing the mass, momentum and energy exchange between the gas and the entrained spray particles are presented in Ref. [4]. The effect of turbulence on the droplet is included by adding a fluctuating velocity to the local mean gas velocity. The collision of droplets is implemented by calculating a collision impact parameter which is compared to a critical collision parameter. The droplet sizes at injection are distributed according to a Rosin-Rammler distribution [8]. The cumulative volume distribution,  $V$  and the corresponding volume distribution,  $dV/dD$  for the Rosin-Rammler distribution are given by the following equations,

$$V = 1 - \exp\left[-\left(\frac{D}{\bar{D}}\right)^q\right] \quad (1)$$

$$\frac{dV}{dD} = \frac{qD^{q-1}}{\bar{D}^q} \exp\left[-\left(\frac{D}{\bar{D}}\right)^q\right] \quad (2)$$

$$\bar{D} = SMD \times \Gamma(1 - q^{-1}) \quad (3)$$

Here  $D$  is the droplet diameter,  $\Gamma$  is the gamma function and  $q$  is the distribution parameter, taken to be 3.5 [9].

The droplet breakup in KIVA-3V is modeled by the Taylor Analogy Breakup (TAB) model, which is based on the analogy between an oscillating droplet and a spring-mass system [10]. In this analogy, the aerodynamic forces on the droplet (due to carrier gas) supply the external force, the surface tension force supplies the restoring force and the liquid viscosity supplies the damping force. Thus, higher aerodynamic forces would favor breakup whereas higher surface tension and liquid viscosity would inhibit the breakup.

In order to match the nozzle configurations and jet orientations with the experiments, CAD models of the injection were used. Figures 1(e) and 1(f) show an example. The SMD for the simulations was taken to be 30 micron, consistent with the experimental data obtained by the Phase Doppler Interferometry [3]. In the experiment, the start of injection (SOI) is at 300° BTDC at 2500 rpm. However, in the simulation, SOI is set at 280.5° BTDC to take into account the 1 ms injector driver pre-charge delay and the 0.3 ms injector opening response delay caused by the solenoid. The duration of injection was matched to the injection pulse width for the 60/5 configuration. Table 1 summarizes the main engine and spray parameters in the reference case.

**Table 1.** Main Engine and Spray Parameters

| Parameter                  | Specification             |
|----------------------------|---------------------------|
| Bore                       | 90.2 mm                   |
| Stroke                     | 105.8 mm                  |
| Compression ratio          | 11:1                      |
| Engine speed & load        | Full Load: 2500 RPM/WOT   |
| Start of injection         | 280.5 BTDC (fourth cycle) |
| Duration of injection      | 67.5 CA                   |
| Number of particles        | 48000                     |
| Shape of injection pulse   | Square                    |
| Injection velocity         | 50 m/s                    |
| Sauter mean diameter (SMD) | 30 $\mu$ m                |

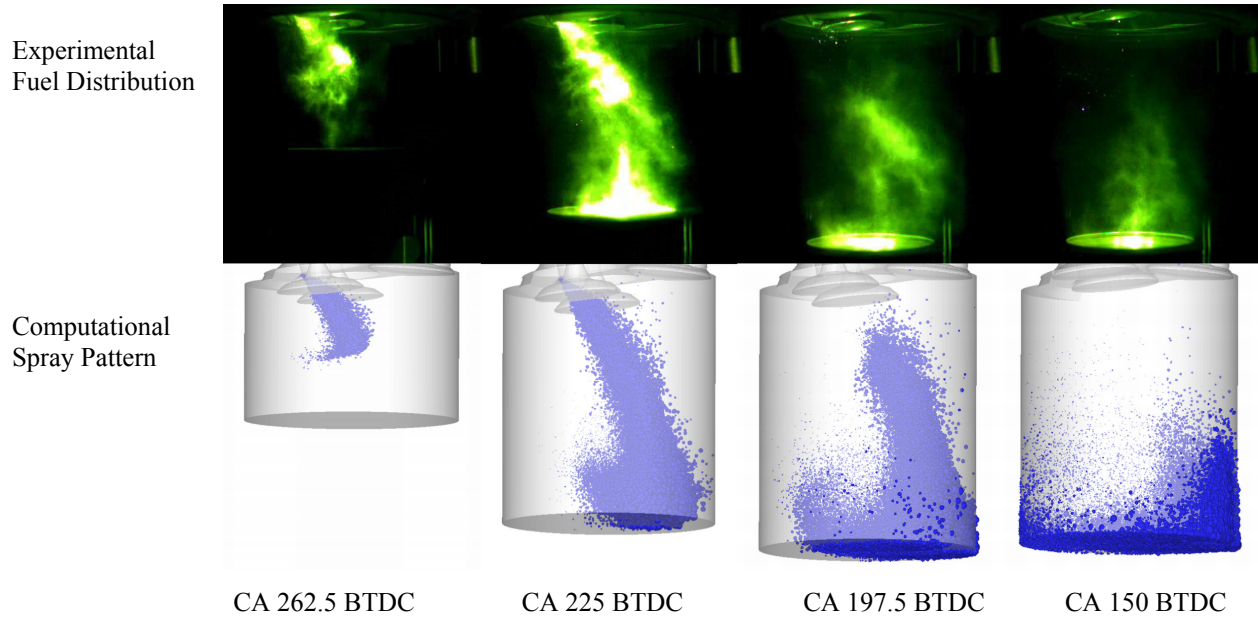
## Results and Discussion

Figure 2 shows the comparison of the fuel distribution images obtained from the optical study with the spray patterns obtained from the numerical simulations. A qualitative visual comparison indicates a good agreement. Figure 3 compares the overall fuel impingement index and the percentage of liquid fuel impinging on the cylinder walls as obtained by the numerical simulations for the 40/0 and 80/10 configurations. Although a very good quantitative comparison is not expected because of different methods employed for the quantification of impingement, it can be seen that the crank angles at which the impingement begins and at which it peaks are almost the same, particularly for the 80/10 configuration. A possible cause for the discrepancies between experimental and numerical results may be the inconsistent illumination in the experiments in areas such as the bottom of the liner wall leading to underestimation or overestimation of the impingement. Nevertheless, the “good” agreement between experimental and computational results in Figures 2 and 3 suggests that the numerical simulations can be used for a better understanding of the effects of different injector configurations and spray patterns on the fuel-air mixing. Some examples are shown below.

Figure 4 shows the predicted fuel impingement on the cylinder walls, piston and valves for various nozzle configurations. The narrower 40/0 spray configuration has the largest impingement on the cylinder walls and piston, while the wider 80/10 configuration yields the least impingement. The 8-hole 60/5 configuration and the 6-hole configuration have intermediate impingements. These results suggest that a wider spray, with a higher offset towards the piston, would have a lower impingement on the cylinder walls, and may mitigate wall film formation. However, as the injector tip is located in the vicinity of the intake valves, the 80/10 configuration also produces a larger fuel impingement on the intake valves as compared to the other narrower spray angle configurations. Figure 4(d) shows the spark-plug wetting for different configurations. As expected, the 80/10 nozzle configuration generates the high-

est liquid fuel concentration in the spark plug area, although the results might become different if splashing of the fuel from the spark plug is included in the model.

Figure 5 shows the predicted mean fuel-air equivalence ratio, calculated on the basis of the total mass of gaseous fuel and oxidizer in the cylinder, for various configurations. The 80/10 configuration has the highest equivalence ratio near the TDC at the end of the compression cycle. The equivalence ratio is comparatively lower for the 60/5 and 40/0 8-hole and 6-hole nozzle configurations. It is to be emphasized here that the reported mean equivalence ratio only indicates the extent of vaporization; a more detailed analysis would be needed for local fuel-air mixing.



**Figure 2.** Comparison of fuel distribution images from the experiment with the predicted spray patterns from the numerical simulation for the 60/5 configuration.

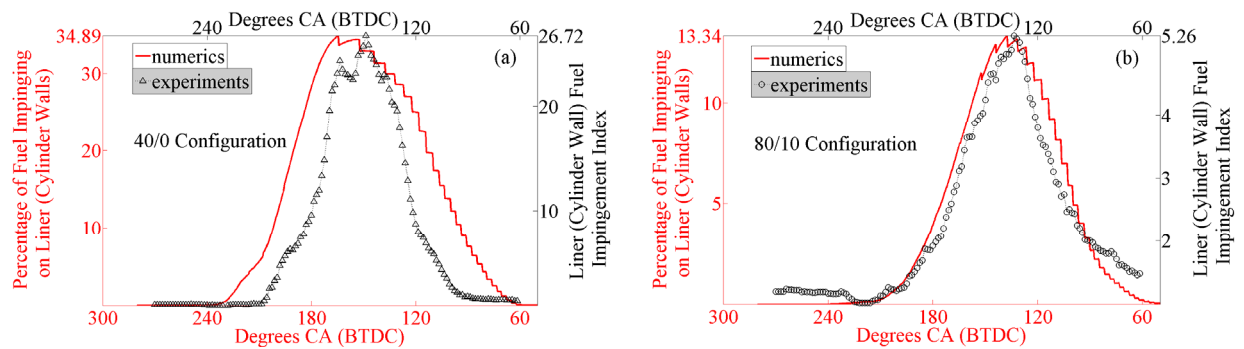


**Figure 3.** Comparison between the percentage of cylinder wall fuel impingement as obtained from the numerical data and the cylinder wall fuel impingement index as calculated from the experimental data at different crank angles (CA). (a) 40/0 injector configuration, (b) 80/10 injector configuration.

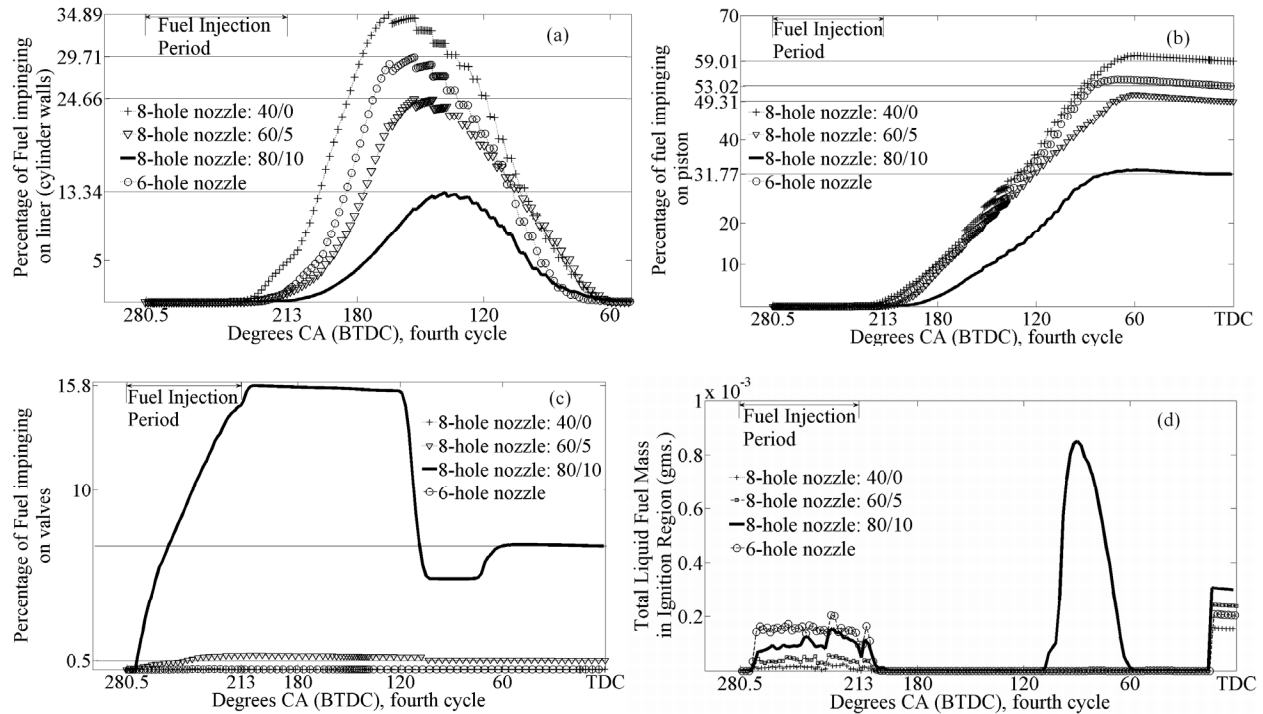


**Figure 4.** The liquid fuel concentration on (a) cylinder walls or liner, (b) piston, (c) valves, and (d) the liquid fuel mass in the ignition region.

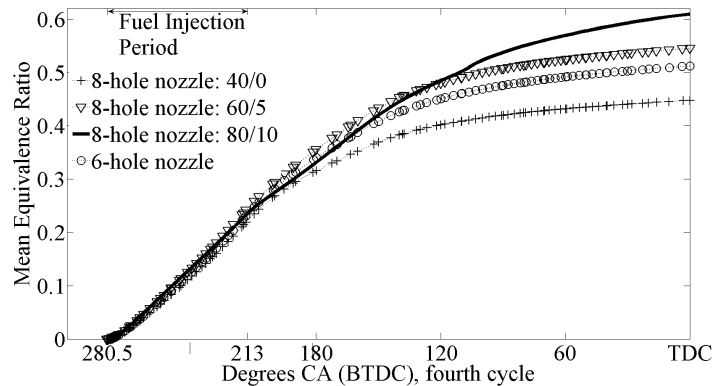


**Figure 5.** Mean equivalence ratio vs. crank angle for different nozzle configurations.

## Conclusions

The data generated from both experiments and simulations have been used for a better understanding of the fuel-air mixing process in a single-cylinder Direct-Injection (DI) gasoline engine. The experimental measurements were performed using a Mie-scattering technique. The numerical simulations were conducted by KIVA-3V. The liquid (droplet) and evaporated (gaseous) fuel concentrations at different locations were calculated from the experimental and numerical data. The results show a reasonably good agreement between the predicted and measured amount of liquid fuel impingement on the solid surfaces. Detailed analysis of the results indicates that (1) the injector spray pattern significantly affects the fuel-air mixture formation process, (2) a wider spray, directed towards the piston, manifests a lower cylinder wall impingement, (3) a wider spray generates a richer fuel-air mixture.

## Acknowledgement

The authors wish to thank the Michigan Economic Development Corporation (MEDC) for their support of this research.

## Nomenclature

|             |                                |
|-------------|--------------------------------|
| <i>BTDC</i> | Before Top Dead Centre         |
| <i>CA</i>   | Crank Angle                    |
| <i>CAD</i>  | Computer-Aided Design          |
| <i>CFD</i>  | Computational Fluid Dynamics   |
| <i>D</i>    | Diameter of individual droplet |
| <i>GDI</i>  | Gas Direct Injection           |
| <i>DI</i>   | Direct Injection               |
| <i>q</i>    | Distribution parameter         |
| <i>LPDI</i> | Low Pressure Direct Injection  |
| <i>RPM</i>  | Revolutions Per Minute         |
| <i>SMD</i>  | Sauter Mean Diameter           |
| <i>SOI</i>  | Start of Injection             |
| <i>TDC</i>  | Top Dead Centre                |
| <i>V</i>    | Cumulative volume distribution |
| <i>WOT</i>  | Wide Open Throttle             |

## References

1. Xu, M., Porter, D., Daniels, C., Panagos, G., Winkelman, J., and Munir, K., *SAE Powertrain and Fluid Systems Conference and Exhibition*, San Diego, USA, October 2002, SAE 2002-01-2746.
2. Xu, M., Low Pressure Direct Injection Engine System, US Patent 6712037, 2003.
3. Hung, D.L.S., Zhu, G.G., Winkelman, J.R., Stuecken, T., Schock, H., and Fedewa, A., *SAE World Conference and Exposition*, Detroit, USA, April 2007, SAE 2007-01-1411.
4. Amsden, A.A., Ramshaw, J.D., O'Rourke, P.J., and Dukowicz, J.K., "KIVA: A Computer Program for Two- and Three-Dimensional Fluid Flows with Chemical Reactions and Fuel Sprays", Los Alamos National Laboratory Report No. LA-10245-MS.
5. Amsden, A.A., "KIVA-3: A KIVA Program with Block-Structured Mesh for Complex Geometries", Los Alamos National Laboratory Report No. LA-12503-MS.
6. Amsden, A.A., "KIVA-3V: A Block-Structured KIVA Program for Engines with Vertical or Canted Valves", Los Alamos National Laboratory Report No. LA-13313-MS.
7. Amsden, A.A., "KIVA-3V, Release 2, Improvements to KIVA-3V", Los Alamos National Laboratory Report No. LA-13608-MS.
8. Baumgarten, C., *Mixture Formation in Internal Combustion Engines*, Springer, 2006, p.91.
9. Han, Z., Parrish, S., and Reitz, R.D., *Atomization and Sprays* 7:663-684 (1997).
10. O'Rourke, P.J., and Amsden, A.A., *International Fuels and Lubricants Meeting and Exposition*, Toronto, Ontario, November 1987, SAE 872089.